Examining Radiation-Induced *In Vivo* and *In Vitro* Gene Expression Changes of the Peripheral Blood in Different Laboratories for Biodosimetry Purposes: First RENEB Gene Expression Study

M. Abend,[a,1,2] C. Badie,[b,2] R. Quintens,[c,2] R. Kriehuber,[e,2] G. Manning,[b] E. Macaeva,[c,f] M. Njima,[d] D. Oskamp,[e] S. Strunz,[g] S. Moertl,[h] S. Doucha-Senf,[a] S. Dahlke,[i] J. Menzel[i] and M. Port[a]

[a] *Bundeswehr Institute of Radiobiology, Munich, Germany;* [b] *Cancer Group, Radiation Effects Department, Centre for Radiation, Chemical and Environmental Hazards, Public Health England, Chilton, United Kingdom;* [c] *Radiobiology and* [d] *Microbiology Units, Institute for Environment, Health and Safety, Belgian Nuclear Research Centre, Mol, Belgium;* [e] *Radiation Biology Unit, Department of Safety and Radiation Protection, Forschungszentrum Jülich GmbH, Jülich, Germany;* [f] *Department of Molecular Biotechnology, Ghent University, Ghent, Belgium;* [g] *Biomathematics and Bioinformatics Unit, Institute of Genetics and Biometry, Leibniz Institute for Farm Animal Biology (FBN), Dummerstorf, Germany;* [h] *Institute of Radiation Biology, Helmholtz Zentrum, Munich, Germany; and* [i] *Medizinische Hochschule Hannover, Hannover, Germany*

Abend, M., Badie, C., Quintens, R., Kriehuber, R., Manning, G., Macaeva, E., Njima, M., Oskamp, D., Strunz, S., Moertl, S., Doucha-Senf, S., Dahlke, S. Menzel, J. and Port, M. Examining Radiation-Induced *In Vivo* and *In Vitro* Gene Expression Changes of the Peripheral Blood in Different Laboratories for Biodosimetry Purposes: First RENEB Gene Expression Study. *Radiat. Res.* 185, 109–123 (2016).

The risk of a large-scale event leading to acute radiation exposure necessitates the development of high-throughput methods for providing rapid individual dose estimates. Our work addresses three goals, which align with the directive of the European Union's Realizing the European Network of Biodosimetry project (EU-RENB): 1. To examine the suitability of different gene expression platforms for biodosimetry purposes; 2. To perform this examination using blood samples collected from prostate cancer patients (*in vivo*) and from healthy donors (*in vitro*); and 3. To compare radiation-induced gene expression changes of the *in vivo* with *in vitro* blood samples. For the *in vitro* part of this study, EDTA-treated whole blood was irradiated immediately after venipuncture using single X-ray doses (1 Gy/min^{-1} dose rate, 100 keV). Blood samples used to generate calibration curves as well as 10 coded (blinded) samples (0–4 Gy dose range) were incubated for 24 h *in vitro*, lysed and shipped on wet ice. For the *in vivo* part of the study PAXgene tubes were used and peripheral blood (2.5 ml) was collected from prostate cancer patients before and 24 h after the first fractionated 2 Gy dose of localized radiotherapy to the pelvis [linear accelerator (LINAC), 580 MU/min, exposure 1–1.5 min]. Assays were run in each laboratory according to locally established protocols using either microarray platforms (2 laboratories) or qRT-PCR (2 laboratories). Report times on dose estimates were documented. The mean absolute difference of estimated doses relative to the true doses (Gy) were calculated. Doses were also merged into binary categories reflecting aspects of clinical/diagnostic relevance. For the *in vitro* part of the study, the earliest report time on dose estimates was 7 h for qRT-PCR and 35 h for microarrays. Methodological variance of gene expression measurements (CV ≤10% for technical replicates) and interindividual variance (≤twofold for all genes) were low. Dose estimates based on one gene, ferredoxin reductase (*FDXR*), using qRT-PCR were as precise as dose estimates based on multiple genes using microarrays, but the precision decreased at doses ≥2 Gy. Binary dose categories comprising, for example, unexposed compared with exposed samples, could be completely discriminated with most of our methods. Exposed prostate cancer blood samples (n = 4) could be completely discriminated from unexposed blood samples (n = 4, P < 0.03, two-sided Fisher's exact test) without individual controls. This could be performed by introducing an *in vitro*-to-*in vivo* correction factor of *FDXR*, which varied among the laboratories. After that the *in vitro*-constructed calibration curves could be used for dose estimation of the *in vivo* exposed prostate cancer blood samples within an accuracy window of ±0.5 Gy in both contributing qRT-PCR laboratories. In conclusion, early and precise dose estimates can be performed, in particular at doses ≤2 Gy *in vitro*. Blood samples of prostate cancer patients exposed to 0.09–0.017 Gy could be completely discriminated from pre-exposure blood samples with the doses successfully estimated using adjusted *in vitro*-constructed calibration curves. © 2016 by Radiation Research Society

Editor's note. The online version of this article (DOI: 10.1667/RR14221.1) contains supplementary information that is available to all authorized users.

[1] Address for correspondence: Bundeswehr Institute of Radiobiology affiliated to University Ulm, Neuherbergstr. 11, 80937 Munich, Germany; email: michaelabend@bundeswehr.org.

[2] These authors contributed equally to this work.

INTRODUCTION

In a large-scale radiological emergency, early diagnosis of exposed individuals would be required to evaluate the

extent of radiation injuries and, when needed, assign an appropriate treatment (*1*). Estimates of the absorbed dose can provide evidence for later occurring acute or chronic health effects. In particular, after high-dose exposure (≥ 2 Gy single whole-body dose) severe acute health effects (acute radiation syndrome) will occur and, therefore, early diagnosis within 1–3 days after exposure is pivotal so that exposed individuals can receive appropriate treatment in specialized clinics as soon as possible. It is important to quickly distinguish among individuals who have been highly exposed from those who think that they have been exposed but who have not ("worried wells") to prevent the nonessential use of limited clinical resources. In the absence of physical dosimetry devices (e.g., in the event of a terrorist attack on the civilian population), biological changes observed after radiation exposure are used to determine individual dose estimates. Among these, scoring of dicentric chromosomes represents the gold standard in biological dosimetry. Although this method has proven to be very reliable and sensitive (*2*), it requires several days (lymphocytes in G_0 phase have to be stimulated to re-enter the cell cycle where they will be arrested in the metaphase *in vitro*) before the dose estimates are available (*3*). However, another biological dosimetry emerging technique is based on gene expression changes observed after radiation exposure. It has already been shown that the expression of several genes has been modulated in a dose-dependent manner after radiation exposure (*4, 5*) and there is growing evidence of the potential for gene expression to be used for high-throughput minimally invasive radiation biodosimetry (*6–10*).

In a recently published study, it was shown that gene expression-based biological dosimetry provided dose estimates that were available within hours after exposure (*11*). It was also reported that gene expression measurements revealed low methodological variation (*11*). These findings represent desirable features for early high-throughput individual dosimetry. However, for successful biodosimetry, two considerations must be taken into account: 1. The interindividual variance of radiation-induced gene expression changes; and 2. Whether currently established and widely used *ex vivo in vitro* blood cell culture models are representative of gene expression changes measured in the peripheral blood *in vivo*.

This study was organized and conducted under the umbrella organization, Realizing the European Network of Biodosimetry (EU RENEB network). In this work, gene expression analysis was performed on blood samples from five healthy donors using an *ex vivo in vitro* whole-blood cell culture model. This model provides information on methodological and interindividual variance in gene expression of certain candidate genes, and can be applied to biodosimetry using different technologies, namely qRT-PCR and microarray. For this work, the gene expression analyses were conducted in four different laboratories, each using either qRT-PCR or microarray. The institution where each laboratory was housed was assigned a number, as follows: 1. Bundeswehr Institute of Radiobiology (IRBBw), Munich, Germany; 2. Centre for Radiation, Chemical and Environmental Hazards, Public Health England (PHE), Chilton, UK; 3. Department of Safety and Radiation Protection, Forschungszentrum Jülich GmbH (FZ), Jülich, Germany/Institute of Genetics and Biometry, Leibniz Institute for Farm Animal Biology (FBN), Dummerstorf, Germany; and 4. Institute for Environment, Health and Safety, Belgian Nuclear Research Centre (SCK CEN), Mol, Belgium. In addition, we also compared radiation-induced gene expression changes measured in *in vivo* exposed blood of four prostate cancer patients undergoing radiotherapy with the measurements generated in *ex vivo in vitro* experiments.

MATERIALS AND METHODS

Blood Sampling, Irradiations and Distribution to Participant Laboratories

For the *ex vivo in vitro* part of the study, 2–3 ml of peripheral blood were drawn from healthy human volunteers and filled into EDTA-coated vials using a Vacutainer® system (BD Biosciences, Heidelberg, Germany). However, prior to the experiment, contributing laboratories received both EDTA-coated and heparin-containing vials to determine which chemistry would work best for our purposes. Fresh blood samples were irradiated at 37°C using single doses of X rays with mean photon energy of 100 keV. X rays were generated using a MG325 generator/control unit and an X-ray tube (Y.TU 320-D03; Yxlon, Hamburg, Germany), which was equipped with a 3 mm beryllium and 3 mm aluminum filter and installed in a Maxishot SPE cabinet (Yxlon). The absorbed dose was measured using a UNIDOS^{webline} dosimeter (type 10021; PTW, Freiburg, Germany). The dose rate was approximately 1.0 Gy/min^{-1} at 13 mA and 240 kV. To permit charged particle equilibrium there must be sufficient material surrounding the blood and the material should be reduced to a minimum to avoid scattered radiation (*2*). For 250 kVp X rays only 1 mm is necessary (*2*). The specimen container wall (blood tubes) met both of these conditions. After irradiation, samples were incubated *in vitro* at 37°C for a certain period of time and lysed cells from these cultures (for details see the Sample Processing and Analysis section) were shipped by overnight courier service under defined conditions according to United Nations regulation 650. Temperature profiles and potential radiation exposures were monitored by adding temperature loggers (TL30; 3M, Neuss, Germany) and film badges (Helmholtz Zentrum Munich, Germany) to the packages. Blood samples were sent to participant laboratories in three phases: 1. We delivered blood samples from two donors (irradiated with 0, 1.5 and 4 Gy) as a pre-experiment for preparation before the study; 2. Then, blood samples from two healthy donors irradiated with 0, 0.25, 0.5, 1, 2, 3 and 4 Gy (total n = 14) were sent for the optional generation of calibration data; and 3. Two weeks later, ten coded blind samples irradiated with 0, 0.1, 0.9, 1.2, 2, 2.5, 2.6, 3.2, 3.7 and 4 Gy [total n = 10, two blood samples from each of 5 donors were irradiated with two different doses (Table 1)] were distributed to participating laboratories for rapid biodosimetry using the same radiation quality and radiation exposure conditions as for the calibration samples.

For the *in vivo* part of the study PAXgene tubes (Qiagen, PreAnalytiX GmbH, Hilden, Germany) were used. About 2.5 ml peripheral blood were taken from five prostate cancer patients before exposure and 24 h after the first radiotherapy fraction of 2 Gy local exposure to the pelvis. Patients were treated with intensity-modulated radiation therapy (IMRT), which is a standard technique of external

TABLE 1
Exposures and Characteristics of Healthy Donors and Prostate Cancer Patients

Ex vivo in vitro part (healthy donors)				
	Donor ID	Age	Gender	Absorbed dose (Gy)
Pre-experiment	1	55	Male	0, 1.5, 4
Calibration samples	1	55	Male	0–4 Gy, n = 7
	2	29	Male	0–4 Gy, n = 7
Blind samples	1	25	Male	0, 2.5
	2	55	Male	0.1, 2.6
	3	29	Female	0.9, 3.2
	4	45	Male	1.2, 3.7
	5	53	Male	2.0, 4.0

			In vivo part (all male, prostate cancer patients)		
			Equivalent total-body blood dose		
	Patient ID	Age	Median (Gy)	Mean (Gy)	Diagnosis, prostate cancer tumor	Comorbidities
Pre-experiment	1	63	0.016	0.33	PCa, pT3 pN1(1/10) M0	Status after hairy-cell leukemia diagnosis 1999 (CR); hypertension.
Blind samples	1	80	0.009	0.25	PCa, cT2b cN0 M0	Hypertension; hyperuricemia.
	2	68	0.013	0.32	PCa, cT2c cN0 M0	Coronary artery disease; status after myocardial infarction 2009; status after apoplexy 2012; diabetes mellitus type 2; peripheral artery disease.
	3	79	0.010	0.25	PCa, cT3-4 cN1 M0	Coronary artery disease; status after myocardial infarction and coronary artery bypass surgery 2009; status after deep vein thrombosis; nephrolithiasis; hypertension.
	4	72	0.017	0.30	PCa, pT3b pN1 (6/22) M0	Nephrolithiasis.

Notes. Patients received IMRT, which is the standard technique for external beam radiation therapy of prostate cancers. Doses for prostate cancer patients represent estimated median and mean equivalent total-body blood doses.

beam radiotherapy used for prostate cancer patients. We used a LINAC with a dose rate of 580 MU/min. The LINAC accelerates electrons on to a tungsten target to produce high-energy photons. The real beam-on time for patients varied from 1 to 1.5 min. For the physical dose reconstructions and the calculation of an equivalent total-body blood dose, the partial-body dose coming from the treatment planning system (Oncentra® 4.1; Elekta, Stockholm, Sweden) was weighted against the whole-body volume to get the average whole-body dose, employing an Alderson RANDO anthropomorphic humanoid phantom (torso duplicate of an average human body). For these calculations it was considered that liver, heart/large blood vessels and lungs together contain 38.5% of the total blood volume (*12*). Other factors such as gender, age, weight and height were not taken into account. It is worth noting that median dose estimates of both approaches, the Alderson RANDO phantom and calculations including individual parameters as shown above (e.g., age, gender, weight and height) appeared comparable (data not shown). Thus, both an unexposed (pre-exposure) and an exposed blood sample were eligible from five prostate cancer patients, which adds up to another 10 blind samples. Details regarding age, gender and estimated whole-body blood dose of the patients are shown in Table 1. These samples were delivered to the two laboratories utilizing qRT-PCR, since only those laboratories could contribute to this part of the study. Sample transport was performed in a similar way as outlined above, but samples were sent separately from the *ex vivo in vitro* study part because of the delayed availability of the patient material. As with the *in vitro* studies two samples from one prostate patient were sent before the main study was performed for preparatory purposes and the remaining four sample pairs were blind-coded and sent at a later time. Laboratories were asked to distinguish between four unexposed and

four exposed samples. Based on their *ex vivo in vitro* calibration curves they were also asked to provide a dose estimate, if possible.

Blood was taken with informed consent and the approval of a local ethics committee.

Sample Processing and Analysis

To perform the *ex vivo in vitro* gene expression assays the irradiated blood samples were diluted with an equal volume of Roswell Park Memorial Institute (RPMI) 1640 medium containing 10% FCS (*13*) and incubated for 24 h at 37°C. The suspension was centrifuged, washed and centrifuged again according to the QIAamp RNA Blood Mini Kit manual. Finally, cells of the pellet were lysed in RLT buffer (QIAamp RNA Blood Mini Kit, Qiagen, Hilden, Germany), stored at −20°C and shipped on wet ice. Microarrays as well as qRT-PCR assays were performed at the laboratories according to established protocols (Tables 2 and 3). Table 3 gives details of RNA isolation, cDNA synthesis and further parameters used by each laboratory.

For the *in vivo* gene expression analysis 2.5 ml of whole blood was collected in PAXgene tubes. The tubes were gently inverted (10 times), stored at room temperature overnight and then stored at −20°C until use. Tubes were blind-coded and shipped on wet ice. In laboratory 2, RNA was extracted according to the PAXgene Blood miRNA Kit (Qiagen). In laboratory 1, PAXgene tubes were thawed, then centrifuged, and the pellet was then washed several times and finally, cells were lysed (Proteinase K) according to the PAXgene manual. Then, the lysate suspension was further processed according to the mirVana™ Kit manual (Life Technologies, Darmstadt, Germany). In short, a lysis/binding solution was added to the suspension, and after administration of homogenate additive and

TABLE 2
General Characteristics of Technical Procedures Utilized and Experiences of the Contributing Institutions

Laboratory number, institution, location	Platform/ chemistry	No. of genes/fit	Gene name	Calibration and blind samples processed	Response
1. IRBBw, Munich, Germany	qRT-PCR (TaqMan)	1, Lin, log scale	FDXR	Separately	First
		1, Lin, log scale	FDXR	Together	Second
2. PHE, Chilton, UK	qRT-PCR (TaqMan)	1, Linear	FDXR	Together	First
		5, Linear or LQ	PHPT1, SESN1, DDB2, CCNG1, CDKN1A	Together	Second
3. FZ, Jülich, Germany/ FBN, Dummerstorf, Germany	Microarrays	16, K-nearest neighbor	e.g., TNFSF4, FDXR, SPATA18, PHLDA3, VWCE, PRICKLE1	Separately	First
		7, LQ	TNFSF4, LGR6, FDXR, SPATA18, DOK7, PHLDA3, VWCE	Separately	First
4. SCK CEN, Mol, Belgium	Microarrays	18, LQ	e.g., DDB2, POLH, MDM2, TNFRSF10B, AEN, EDA2R, RPS27L	Together	First
		247, SVM, exons	e.g., ASTN2, MAMDC4, PHPT1, TNFRSF10B	Together	Second
		247, NNs, exons			
		50, SVM, genes	e.g., PLK3, GADD45A, LMNA, RGL1, JUN	Together	Second
		50, NNs, genes			

Notes. Contributing groups were asked to report their dose estimates as soon as possible, which is indicated as their first response. Later and before sharing the true doses we allowed further reports on dose estimates, which is indicated as their second response.

acid-phenol:chloroform and centrifugation, the RNA was extracted from the upper phase. After addition of ethanol to this RNA-containing suspension the solution was placed on a silica membrane column. After several washing steps, DNA residuals were digested on the membrane (RNase-free DNase Set, Qiagen), which was then washed, and RNA was eluted and converted into cDNA (see Table 3 for qRT-PCR details).

We applied the WEKA data mining[3] for the microarray analysis and employed the SMOreg classifier, which implements a support vector machine (SVM) for regression algorithm and the multilayer perceptron classifier, which implements a neural network (NN) algorithm. To enhance the performance of these learning algorithms we applied two filters: the principal component analysis and correlation-based filters. Principal components analysis produces the combinations of attributes that contribute to the best prediction. It reduces the dimensionality of the data matrix by finding combinations of attributes that account for as much of the variance in the original attributes as possible while remaining mutually uncorrelated. On the other hand, the correlation-based filter method uses a correlation-based heuristic to determine the value of a subset of attributes by considering the individual predictive ability of each feature along with the degree of redundancy between them. This method produces a subset of attributes that are highly correlated with the class (dose) while having low intercorrelation. To train and test our machine-learning models and reduce the chance of overfitting we used cross validation with tenfolds. Thus, the dataset was split into 10 parts. The first 9 parts were used to train the algorithm and the 10th was used to assess the algorithm. We used the dataset in which the dosage was known to train and then applied the trained model onto the dataset with unknown doses for prediction.

[3] Mark Hall, Eibe Frank, Geoffrey Holmes, Bernhard Pfahringer, Peter Reutemann, Ian H. Witten (2009); The WEKA Data Mining Software: An Update; SIGKDD Explorations, Volume 11, Issue 1.

Collection of Biodosimetry Data and Survey Information

Two data sheets were provided to each participant laboratory, one to report the triage dose estimates of blind samples as soon as possible and the other to provide the complete data, including calibration data and details concerning the technical performance. The time between the arrival of the samples at the participating laboratory (courier report) and the return of the dose estimates of blind samples to the organizer via email was documented. Further information about each laboratory was collected as follows: 1. Number of exercises the laboratory had participated in prior to the RENEB study; 2. Their own judgment of the laboratory's proficiency level for each assay; 3. The length of time that each method had been established; 4. The length of time that each method had been used for biodosimetry; and 5. The level of priority given to the analysis of the samples during daily business.

Statistical Methods

The precision of reported dose estimates was measured by calculating the mean of the absolute differences (MAD) of estimated doses to their corresponding true doses. Finally, we merged doses into binary categories reflecting clinically/diagnostically/epidemiologically relevant aspects and assessed the agreement between the true doses and the reported dose estimates among the binary categories. Those categories were:

- Never versus ever single radiation exposure (0 vs. ≥ 0.1 Gy), established to prevent the unnecessary use of clinical resources by the "worried well".
- Marginal versus higher single radiation exposures (≤ 0.2 vs. >0.2 Gy). At low-level doses (≤ 0.2 Gy), stochastic effects (e.g., tumorigenesis) in adults might occur. No acute clinical interventions are required. At exposures >0.2 Gy stochastic effects are expected and become detectable years after exposure using

TABLE 2
Extended.

No. of previous exercises	Laboratory specialized in biodosimetry	Method established (month)	Method established for biodosimetry purposes (month)	RENEB samples processed with
1	Yes	90	60	Priority
1	Yes	80	55	Priority
0	No	96	48	Priority
	No	96	48	
0	No	95	56	Priority

conventional epidemiological methods. At higher doses, deterministic effects (e.g., acute radiation syndrome) will occur as well and here clinical interventions might be indicated.
- Media versus higher single radiation exposure ($\leq$2 vs. >2 Gy) for triage purposes in the case of limited clinical resources.

Sensitivity, specificity, accuracy, predictive value positive (PVP) and predictive value negative (PVN) were assessed on the basis of the estimated doses compared to the known doses and a 2×2 contingency table was applied, which was comprised of: true positive (TP), true negative (TN), false positive (FP) and false negative (FN). The corresponding percentages were calculated for the following: accuracy $=$ (TP $+$ TN) $\times$ 100/(total); sensitivity $=$ TP $\times$ 100/(TP $+$ FN); specificity $=$ TN $\times$ 100/(TN+FP); PVP $=$ TP $\times$ 100/(TP $+$ FP); and PVN $=$ TN $\times$ 100/(TN $+$ FN).

Descriptive statistics were calculated in Microsoft Excel. An insignificant association of different donors (blind samples, $P =$ 0.98) on gene expression-based dose estimates (dependent variable) was calculated in linear regression models adjusted for the true dose due to its collinearity with the donors (Pearson correlation coefficient $= 0.33$, $P < 0.0001$). Alterations in ferredoxin reductase (FDXR) gene expression (unexposed) due to gender, age and association with certain blood cell counts (hemoglobin, leucocytes, thrombocytes and lymphocytes) as an indicator of the origin of the expressed genes could be performed on only a small data set because of missing blood cell counts (n $=$ 3–8) or data available for males only employing linear regression models. Therefore, gender dependency could not be examined; associations of gene expression with blood cell counts were insignificant and a weak association with age (0.02) was found. Separation of exposed from unexposed prostate cancer blood samples based on FDXR gene expression was analyzed employing a two-sided Fisher's exact test on the corresponding frequency table. The analytical statistics were performed using SAS® (v.9.2; SAS Institute Inc., Cary, NC). Graphs were created using Sigma Plot 9.0 (Jandel Scientific, Erkrath, Germany).

RESULTS

Ex Vivo In Vitro Study Part

Number of participating institutions, contributions and dose estimates. Of the four participating institutions (Table 2), one experienced technical difficulties with a calibration sample, when one of the plastic tubes arrived cracked; thus, the RNA sample from one donor was lost, leaving six instead of seven samples from one donor eligible for constructing the calibration curve. Laboratory 1 ran qRT-PCR gene expression assays of calibration and blind samples together and separately (also, two different macros for dose estimates were employed) and three different genes and corresponding dose estimates were employed by the qRT-PCR laboratory 2 (total contributions of qRT-PCR laboratories was n = 6). The two laboratories using microarrays estimated the dose based on seven different algorithms. Both laboratories employed linear-quadratic (LQ) equations on a previously identified gene set consisting either of 7 genes (laboratory 3) (*9, 10*) or 18 genes (laboratory 4).[4] Both microarray laboratories also utilized several other tools for dose estimation, namely a k-nearest neighbor classification (laboratory 3) and SVM and NN classifications, which were employed for gene expression measurements generated from exons and genes (laboratory 4).

Therefore, four institutions provided 13 contributions (6 from qRT-PCR and 7 from microarray laboratories), and thus 130 dose estimates were analyzed. All participant laboratories provided survey information concerning laboratory organization and assay performance (Table 2).

Sample delivery and report time of dose estimates. The transport temperature logger placed in each box detected temperature fluctuations typically ranging between 0–8°C during the shipment of the calibration as well as the blind samples. With one exception, film badge dosimeters provided no indication of undesired additional radiation exposure of the samples during the transport. As for the one exception, an additional exposure of 0.1 mSv was detected in the three pre-experiment samples delivered to Belgium.

Transit time did not exceed 24 h irrespective of the location of the laboratories, which were in Germany, UK and Belgium (Table 4). A delay ranging from 5 min up to 1:33 h was observed between the arrival of the samples at the institutional post offices and the delivery to laboratory personnel. After arrival of blood samples at the participating laboratories, the earliest report on dose estimates was submitted 6:46 h later for laboratories using qRT-PCR and 34:52 h later for laboratories using microarrays. The overall report time ranged between 0.3 and 2 days.

Pre-experimental results. Laboratories received irradiated blood samples treated with EDTA and lithium-heparin (3 of each) to identify the most appropriate blood anticoagulant for use in further experiments. RNA integrity number

---

[4] Macaeva *et al.* (submitted for publication).

TABLE 3
Methods Used by Contributing Laboratories

	qRT-PCR	
	Laboratory 1: IRBBw, Munich, Germany	Laboratory 2: PHE, Chilton, UK
RNA isolation		
Isolation kit	QIAamp RNA Blood Mini Kit	QIAamp RNA Blood Mini Kit
DNA digestion during isolation	RNase-free DNase Set	RNase-free DNase-Set
Template eluted in:	RNase-free water	TE or RNase-free water
Quality control		
RNA integrity number	Yes	No, agarose gel
Concentration	Yes (NanoDrop™)	Yes (NanoDrop)
A260/280	Yes	Yes
A260/230	Yes	Yes
Check DNA contamination	Conventional PCR with β-actin primer and HotStar MasterMix, 30 cycles.	-RT control
cDNA synthesis		
Kit/MasterMix	High capacity cDNA archive kit	High capacity cDNA archive kit
PCR protocol	$1\times$/25°C/10 min, $1\times$/37°C/120 min	$1\times$/25°C/10 min, $1\times$/37°C/120 min, $1\times$/85°C/5 min
Quality control	18S rRNA Ct	HPRT1 Ct
qRT-PCR		
Kit/MasterMix	TaqMan Universal Master Mix	TaqMan, PerfeCTa®, MultiPlex qPCR SuperMix
fp/rp/probe	GADD45A, no. Hs00169255_m1	PCNA, PHPT1, TIGAR, CCNG1, DDB2, FDXR, GADD45A, MDM2
	BAX, no. Hs00180269_m1 DDB2, no. Hs00172068_m1 CDKN1A, no. Hs00355782_m1	
Cycles	$1\times$/50°C/2 min, $1\times$/95°C/10 min, $40\times$/95°C/1 min and 60°C/1 min	2 min, $40\times$/95°C/10 s and 60°C/1 min
Detection system	GeneAmp® 7900	Rotor-Gene 6000
Fixed/variable threshold	Automatic	Fixed
Normalization	Human 18S rRNA	HPRT1
Quantification method	DD approach	2 Standard curves. Relative quantification
Quality control		
Standard curve	Yes	Yes
Slope	Yes	Yes
r2	Yes	Yes
18S rRNA Ct	Yes	HPRT1, (-)RT and NTC
	Microarrays	
	Laboratory 3: FZ, Jülich, Germany/FBN, Dummerstorf, Germany	Laboratory 4: SCK CEN, Mol, Belgium
RNA isolation		
Isolation kit	RNeasy® Mini Kit	QIAamp RNA Blood Mini Kit
DNA digestion during isolation	No	No
Template eluted in	RNase-free water	RNase-free water
Quality control		
RNA integrity number	Yes	Yes
Concentration	Yes (NanoDrop)	Xpose™
A260/280	Yes	Yes
A260/230	Yes	Yes
Check DNA contamination	No	No
Microarrays		
Microarray type	44k Whole-human genome, G4112F	Human gene 1.0 ST
RNA amount used for cRNA synthesis		0.25 μg
cRNA amount used for cDNA synthesis		10 μg
RNA amount used for cDNA synthesis	0.4 μg	
cDNA amount used for cRNA synthesis	0.4 μg; 1.65 μg per array	
Number of interrogated genes	19,596	28,536
Number of probe sets	>41,000 transcripts	253,002
Probe summarization and probe set normalization algorithm	Feature Extraction software (v.9.5.1;); processed signal values were log2-transformed, median-normalized.	Robust multichip analysis

Note. Details on algorithms for analysis of microarray data from Belgium were reported by Macaeva *et al*. (submitted for publication).

TABLE 4
Documented Times for Blood Sample Mail Delivery and Dose-Estimate Reporting for Each Laboratory

Laboratory ID	Platform	Transit time: Germany to destination	Transit time: institutional post office to laboratory	Time: from laboratory work to dose estimate report
1	qRT-PCR	NA	NA	9 h, 15 min
2	qRT-PCR	21 h, 56 min	1 h, 33 min	6 h, 46 min
3	Microarray	22 h, 45 min	30 min	34 h, 52 min
4	Microarray	22 h, 09 min	5 min	45 h, 34 min

(RIN) values and the total amounts of isolated RNA on average appeared comparable for both blood anticoagulants (Table 5). However, samples treated with EDTA, on average, showed lower cycle threshold (Ct) values (surrogate for RNA copy numbers) for the candidate genes as well as a larger linear dynamic range of the Ct values over the given dose range (0–4 Gy), thus allowing for a better prediction of the dose based on RNA copy number changes (Table 5). Therefore, peripheral blood collected in EDTA tubes was used throughout the entire study.

Calibration samples and selection of candidate genes. Quality checks performed at the different laboratories indicated successful isolation of sufficient amounts of high-quality RNA from lysed cells delivered in RLT buffer (Table 6). Average total RNA amount was 1.9 μg (±1.1 μg) and the mean RIN was 7.7 (±0.9) in laboratories 1, 2 and 4, while approximately 3–5 times more RNA with slightly lower but sufficient RIN was isolated in laboratory 3 where samples were processed without a DNA digestion step (Table 6). The total amount of isolated RNA decreased with increasing dose in donor 2 but not in donor 1, while RIN values appeared to be unaffected (RIN difference per laboratory between donors 1 and 2 over all samples was generally <0.5). A similar pattern was found for the blind samples (data not shown).

We examined the precision of qRT-PCR gene expression measurements by performing technical replicates in duplicate (laboratory 1) and triplicate (laboratory 2). For the microarrays, no replicate measurements of calibration samples were available. The coefficient of variation [(CV) standard deviation relative to the mean RNA copy number] for almost all measurements did not exceed 10% for all genes in laboratory 1 and 20% for almost all measurements in laboratory 2 (Fig. 1A). The corresponding interindividual variance was ≤2.5-fold for all genes in both laboratories

(Fig. 1B). *FDXR* appeared superior over all the examined genes due to the low CV values (≤3.2% for all measurements, mean = 1.5% in laboratory 1) and low interindividual variance in gene expression measured among healthy donors (≤1.4-fold for all measurements and mean = 1.2-fold in laboratory 1). These values were comparable to the housekeeping genes utilized, such as 18S rRNA (mean CV = 0.7% and mean 1.3-fold interindividual difference) in laboratory 1 and HPRT1 (mean CV = 7.0% and 1.1-fold interindividual difference) in laboratory 2.

Calibration curves with Ct values plotted versus dose on a linear scale provided a coefficient of determination (r^2) ranging between 0.82–0.94 in laboratory 1 (Fig. 2A) assuming a LQ dose-response relationship for all six genes. However, the range of Ct values of *FDXR* exceeded 4 log scales (inverse log2-transformed data) compared to, e.g., PCNA (about 2 log scales), suggesting a better assessment of the dose based on gene expression changes when using *FDXR*. For this reason, *FDXR* alone was used to build the calibration curve in laboratory 1 and coefficient of determination increased up to 0.98 after log transformation of dose on the x-axis (Fig. 2B). Measurements of *FDXR* in the 5 healthy donors providing the blind samples as well as in the five prostate cancer patients corresponded to these results. Calibration curves in laboratory 2 showed almost similar characteristics with coefficient of determination ranging between 0.88–0.96 for mean gene expression values of six genes and a LQ dose-response relationship of normalized gene expression values depicted on a linear scale (Fig. 2C). For dose estimates of blind samples, calibration curves using *FDXR*, PHPT1 and DDB2 provided the best results for laboratory 2. The microarray laboratories employed LQ equations on a previously identified gene set consisting of either 7 genes (laboratory 3) or 18 genes (laboratory 4). Laboratory 3 employed these already

TABLE 5
Comparison on RNA and qRT-PCR Gene Expression Characteristics Examined on Blood Samples Using Either EDTA or Lithium Heparin-Coated Blood Tubes

Characteristics	EDTA	Heparin	Practical preference
RNA integrity number	**8.3** ± 1.1; 6.2–10.0	**7.8**, ± 1.5; 5.2–9.4	Sufficient and comparable for both methods
Total RNA amount isolated (μg)	**2.6** ± 1.0; 1.4–4.6	**2.4**, ± 2.0; 0.4–7.0	Sufficient and comparable for both methods
Occurrence raw Ct values	EDTA earlier: **1.1**; ± 0.8; 0.1–2.7		Within the linear dynamic range of both methods
Dose (0–4 Gy) dependent differences of Ct values	**2.8** ± 0.4; 2.3–3.3	**2.1** ± 0.8; 0.4–3.2	**Better discrimination of exposure possible**

Note. Values in bold represent means ± standard deviation and the range (min–max) is given as well.

TABLE 6
Laboratory Intercomparison of RNA Quantity and Quality Isolated from 14 Blood Samples (Calibration Samples)

Donor ID	Dose (Gy)	Laboratory 1		Laboratory 2		Laboratory 3		Laboratory 4	
		Total RNA (µg)	RIN[a]	Total RNA (µg)	RIN[a]	Total RNA (µg)	RIN[a]	Total RNA (µg)	RIN[a]
1	0	1.3	8.2	6.5	7.9	2.6	7.2	2.0	7.4
1	0.25	2.1	8.8	3.1	7.2	7.7	6.5	3.3	8.6
1	0.5	1.9	9.0	2.6	7.5	7.2	8.0	4.0	9.5
1	1	1.9	8.6		-	7.4	6.7	2.5	9.1
1	2	1.6	8.4	1.9	7.0	7.5	6.1	2.5	9.0
1	3	1.8	8.7	2.1	7.5	6.8	6.8	2.7	9.0
1	4	1.8	8.6	1.5	7.5	7.5	7.8	3.0	9.6
2	0	1.6	9.2	1.6	7.8	10.2	8.3	2.3	8.3
2	0.25	1.4	8.3	1.4	7.4	10.5	7.0	2.2	8.3
2	0.5	1.1	8.3	1.2	7.1	7.8	5.9	2.1	8.5
2	1	0.7	8.7	1.4	6.7	5.9	6.3	1.7	7.5
2	2	0.9	8.4	1.1	7.0	5.2	5.6	1.9	6.8
2	3	0.6	8.1	0.5	6.6	6.4	6.4	1.0	6.0
2	4	1.1	8.2	1.0	6.7	7.8	5.7	1.3	6.6

[a] RIN = RNA integrity number.

established calibration curves for dose estimation of the blind samples and laboratory 4 used the provided calibration samples to develop corresponding calibration curves with eight of these calibration curves, as shown in Fig. 2D. The coefficient of determination typically ranged between 0.64–0.81 (Fig. 2D). Due to technical problems the gene expression values at 1 Gy are missing. For the dose estimation of blind samples, the microarray laboratories used e.g., the mean of the predictions for all genes of their gene sets, but when a gene predicted an outlying dose (more than 3 standard deviations different from the mean) this prediction was not taken into account.

Dose estimates performed on ex vivo in vitro irradiated blind samples. A comparison of reported dose estimates versus the true doses showed both an increasing variation of dose estimates for doses >2 Gy and a corresponding increased number of measurements lying outside the recommended 0.5 Gy interval for triage dosimetry (Table 7). This was observed for both qRT-PCR and microarrays and corresponded to MADs of 0.1–0.3 Gy at true doses ≤2 Gy and increased MADs of 0.7–2.0 Gy at true doses lying between 2–4 Gy. Most dose estimates (2–5 out of 5) lying outside the recommended 0.5 Gy interval were registered at true doses ranging between 2–4 Gy, while at true doses ≤2 Gy only 0–1 out of up to 5 measurements were outside of this interval. The imprecise dose estimates at true doses >2 Gy could be overcome with another method used by laboratory 4 (see the last two contributions using SVMs and NNs on genes, Table 7). In return, the MADs for these contributions increased to values of 0.9–1.0 at true doses ≤2 Gy and 4 out of 5 dose estimates were outside the 0.5 Gy intervals.

To address the clinical/diagnostic/epidemiological relevance, we also divided gene expression-based dose estimates into binary categories. Irrespective of the methodology, an almost complete separation of unexposed versus exposed individuals as well as individuals exposed to
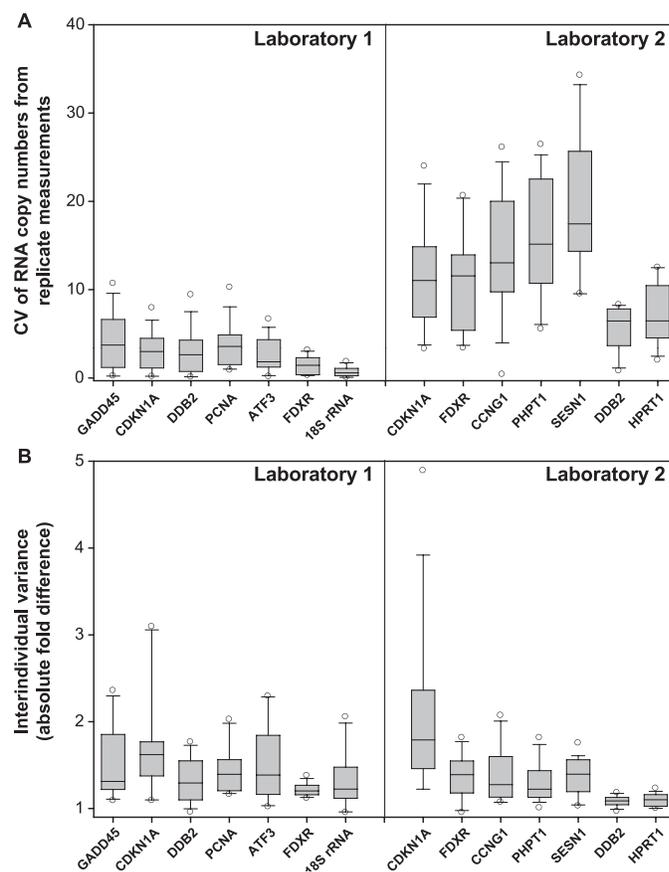
FIG. 1. Panel A depicts coefficient of variation (CV) of RNA copy numbers from technical replicate qRT-PCR measurements and panel B reflects interindividual fold-differences in gene expression among two donors. These measurements were performed in two different laboratories (laboratory 1, left side; laboratory 2, right side) utilizing material from two donors, which were examined using 14 genes. CV and fold-differences between two donors were calculated per gene and for each dose (n = 7) and technical replicate (n = 2 in laboratory 1; n = 3 in laboratory 2), resulting in 14 and 21 measurements for interindividual fold-differences in laboratories 1 and 2, respectively, and 14 measurements for CVs in both laboratories.
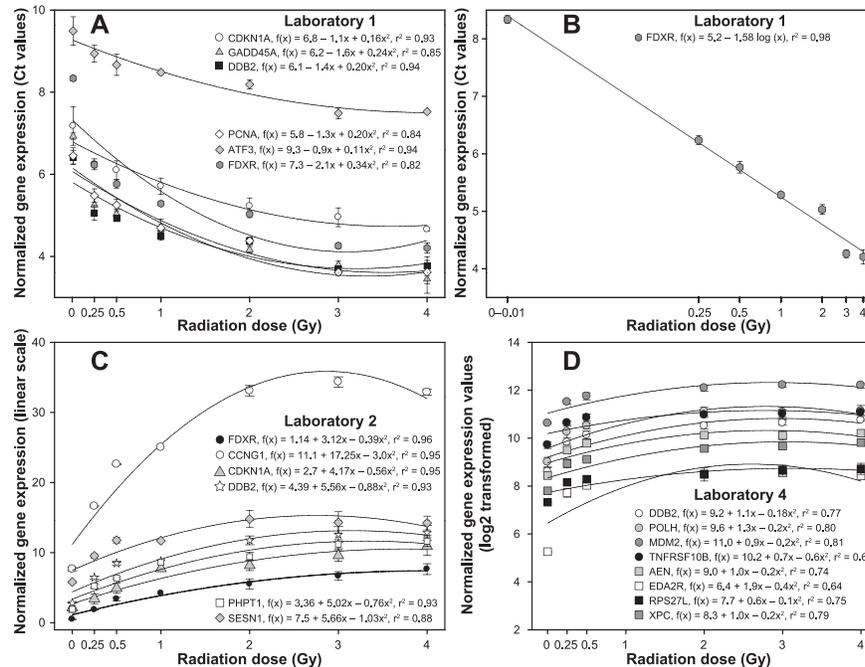
FIG. 2. Calibration curves are shown from the qRT-PCR laboratories 1 (panels A and B) and 2 (panel C) and from the microarray laboratory 4 (panel D). Data points are fitted by a regression line of first (panel B) or second order (panels A, C and D). Symbols represent mean gene expression values from two donors with measurements either performed once (laboratory 4, $n = 2$) in duplicate (laboratory 1, $n = 4$) or triplicate (laboratory 2, $n = 6$). Error bars represent the standard error of mean and are visible when greater than the symbols. After log transformation of dose, *FDXR* was chosen as the only candidate gene for dose estimation in laboratory 1, due to the large Ct range of dose-dependent changes of *FDXR* gene expression and the coefficient of determination of 0.98 (panel B). Gene expression at 0 Gy was depicted at a dose of 0.01 Gy on the log x-scale for visualization purposes.

doses ≤ 0.2 Gy versus higher doses could be achieved (Table 8).

In Vivo Study Part (Prostate Cancer Patients)

As shown in Fig. 3, the four pre-exposure blood samples (white triangles) and the four blood samples taken 24 h after the first radiotherapy fraction from the same prostate cancer patients (dark triangles) could be completely distinguished based on the normalized *FDXR* Ct values in both qRT-PCR laboratories. Based on the 4 highest and the 4 lowest *FDXR* Ct values it was possible to distinguish unexposed from exposed samples with 100% sensitivity, specificity and 100% PVP and PVN (Table 9; $P < 0.03$). All Ct values generated from *in vivo* blood samples were out of the range of the unexposed *ex vivo in vitro FDXR* values of the calibration curve, indicating a discrepancy between the *in vivo* and *in vitro* measurements. When using the *in vitro* calibration curves, negative dose estimates would be calculated based on the *in vivo FDXR* values. Since Ct values (Fig. 3A) represent inverse log2-transformed RNA copy numbers, the *in vitro* data of the calibration curve (gray circles) reveal higher RNA copy numbers than the *in vivo* data, which is also reflected in Fig. 3B representing gene expression values on a linear scale. In detail, the mean *FDXR* Ct value of the unexposed prostate cancer patients' blood samples was 11.01, while *ex vivo in vitro* cultured blood samples showed mean Ct values of 8.22, resulting in

a 6.9 times ($6.9 = 2^{11.01-8.22}$) higher expression in the latter, as measured in laboratory 1. In laboratory 2 this difference was measured as 2.3-fold (Fig. 3B). After correcting for the decreased expression of *FDXR in vivo* over the cell culture system and multiplying the *in vivo* gene expression by a factor of 6.9 for laboratory 1 (Fig. 3A) and 2.3 for laboratory 2 (Fig. 3B), we calculated dose estimates using the *in vitro*-generated calibration curve with results being in close proximity to the physical dose estimates (Table 9). Dose estimates based on *FDXR* gene expression measured in both qRT-PCR laboratories were in close proximity to each other and were systematically higher (800 and 713% in laboratories 1 and 2, respectively) compared to median physical dose estimates, and smaller (33 and 30% in laboratories 1 and 2, respectively), but closer to the mean physical dose estimates (Table 9). All dose estimates ranged inside the ± 0.5 Gy uncertainty interval. Dose estimates in laboratory 1 were less precise when using other gene targets such as GADD45 or PCNA, characterized by higher interindividual variance, as was previously shown *in vitro* (Fig. 1). As a result, it was more difficult to discriminate exposed from unexposed prostate cancer patient samples when using GADD45 or PCNA in laboratory 1 (Table 9). In laboratory 2 other genes (PHPT1, DDB2, CCNG1) also allowed for correct discrimination between unexposed and exposed samples, based on the four lowest and the four highest gene expression values measured. However, the

TABLE 7
Reported Dose Estimates from Laboratories Running qRT-PCR or Microarrays for Each Sample Irradiated with a Known (True) Dose

	True dose for each sample (Gy)									
	0	0.1	0.9	1.2	2.0	2.5	2.6	3.2	3.7	4.0
qRT-PCR: laboratory contribution										
Laboratory 1				Reported dose estimates (Gy)						
FDXR, macro 1	0.0	0.2	0.4	1.2	1.9	2.0	**1.6**	**1.7**	**1.2**	**2.0**
FDXR, macro 2	0.0	0.1	0.4	1.1	2.0	2.1	**1.6**	**1.7**	**1.2**	**2.0**
FDXR, calib + blind samples together, automatic threshold	0.0	0.2	0.5	**1.8**	2.4	**5.8**	**3.6**	**1.9**	**2.5**	**4.7**
Laboratory 2										
FDXR	0.0	0.04	0.5	1.7	1.7	2.5	2.3	**1.8**	4.1	**2.7**
PHPT1	0.0	0.1	1.1	**2.5**	2.1	**1.7**		**2.2**		**2.0**
DDB2	0.0	0.1	1.1	1.6	2.0	2.0		**1.9**	2.5	
[a]MAD (Gy)	0.0	0.1	0.3	0.5	0.2	0.9	0.8	1.4	1.6	1.6
	(0.0–0.0)	(0.0–0.1)	(0.2–0.4)	(0.0–1.3)	(0.0–0.4)	(0.0–3.3)	(0.3–1.0)	(1.0–1.5)	(0.4–2.0)	(0.7–2.0)
No. of measurements out of ±0.5 Gy	0	0	0	2	0	2	3	6	4	5
Microarrays: laboratory contribution										
Laboratory 3				reported dose estimates (Gy)						
k-nearest neighbor	0.0	0.3	1.0	**2.0**	2.0	**4.0**	**2.0**	**2.0**	4.0	**2.0**
LQ regression analysis	0.0	0.4	1.2	**2.0**	2.2	**4.0**	**1.9**	**2.4**	3.4	**2.5**
Laboratory 4										
LQ regression	0.0	0.2	1.0	1.2	**1.4**	**1.7**	**1.9**	**1.6**	**1.5**	**1.6**
SVM, exons	0.0	0.0	**2.0**	1.2	2.2	2.7	3.0	3.4	**2.5**	**2.1**
NN, exons	0.0	0.0	**2.0**	1.1	2.3	2.7	3.1	3.4	**2.5**	**2.0**
SVM, genes	**0.8**	0.1	**2.5**	**2.5**	**2.7**	2.9	2.6	3.5	**3.1**	**3.4**
NN, genes	**0.8**	0.1	**2.7**	**2.6**	**2.9**	**3.1**	2.9	3.7	3.2	3.5
Laboratories 3 and 4, contributions 1–3										
[a]MAD (Gy)	0.0	0.2	0.5	0.4	0.3	0.8	0.6	0.8	1.0	2.0
	(0.0–0.8)	(0.0–0.3)	(0.1–1.1)	(0.0–1.4)	(0.0–0.9)	(0.2–1.5)	(0.4–0.7)	(0.2–1.6)	(0.3–2.2)	(1.5–2.4)
No. of measurements out of ±0.5 Gy	0	0	2	2	1	3	3	3	3	5
Laboratory 4, contributions 4–5										
[a]MAD (Gy)	0.8	0.0	1.7	1.3	0.8	0.5	0.2	0.4	0.6	0.5
	(0.8–0.8)	(0.0–0.0)	(1.6–1.8)	(1.3–1.4)	(0.7–0.9)	(0.4–0.6)	(0.0–0.3)	(0.3–0.5)	(0.5–0.6)	(0.5–0.6)
No. of measurements out of ±0.5 Gy	2	0	2	2	2	1	0	0	1	1

Notes. MAD values (Gy) are calculated per laboratory contribution (right side of table) and per true dose (ascending order, lower sections of table). The min-max MAD values are provided in parenthesis. Dose estimates that do not fall into the ±0.5 Gy uncertainty interval accepted for triage dosimetry are indicated in bold and the total shown per laboratory contribution and per true dose. These two measures of dose precision are examined for true doses ≤2 Gy, 2.5–4 Gy and all doses together. Missing dose estimates for laboratory 2 were caused by technical difficulties. SVM = support vector machine. NN = neural network. LQ = second order regression.

gene expression differences between both groups were very small and as a consequence all exposures resulted in 0 Gy dose estimates using the linear-quadratic fits of the calibration curves of laboratory 2 shown in Fig. 2.

DISCUSSION

Different candidate genes were reported to be suitable for biological dosimetry in multiple publications, but little is known about their applicability in different exposed individuals. To assess the impact of interindividual gene expression variation on the precision of dose estimates we irradiated blood samples from five healthy donors, cultivat-ed the blood *in vitro* for 24 h, distributed the blind-coded samples to four laboratories and compared the provided dose estimates with the true doses. Dose estimates based on radiation-induced alterations in expression of the *FDXR* gene in particular were precise. This can be explained by the low methodological as well as the lowest interindividual variance measured among all 12 genes examined using qRT-PCR. *FDXR* encodes a mitochondrial flavoprotein that initiates electron transport for cytochromes P450 receiving electrons from NADPH. The gene is regulated by the p53 family and sensitizes cells to oxidative stress-induced apoptosis (*14*). It is apparent that this pathway is particularly sensitivity to radiation exposure and even more tightly and

TABLE 7
Extended.

	MAD (Gy)			No. of measurements out of ±0.5 Gy		
≤2 Gy	2.5–4 Gy	All		≤2 Gy	2.5–4 Gy	All
0.1 (0.0–0.5)	1.5 (0.5–2.5)	0.8 (0.0–2.5)		0	4	4
0.1 (0.0–0.5)	1.5 (0.4–2.5)	0.8 (0.0–2.5)		0	4	4
0.1 (0.0–0.4)	1.5 (1.0–3.3)	0.9 (0.0–3.3)		1	5	6
0.3 (0.0–0.5)	0.7 (0.3–1.4)	0.5 (0.0–1.4)		0	2	2
0.3 (0.0–1.3)	1.3 (0.8–2.0)	0.7 (0.0–2.0)		1	3	4
0.1 (0.0–0.4)	1.0 (0.5–1.3)	0.5 (0.0–1.3)		0	2	2
0.2 (0.0–0.8)	1.1 (0.3–1.5)	0.7 (0.0–1.5)		1	4	5
0.3 (0.0–0.8)	1.0 (0.3–1.5)	0.7 (0.0–1.5)		1	4	5
0.2 (0.0–0.6)	1.5 (0.7–2.4)	0.7 (0.0–2.4)		1	5	6
0.3 (0.0–1.1)	0.8 (0.2–1.9)	0.5 (0.0–1.9)		1	2	3
0.3 (0.0–1.1)	0.8 (0.2–2.0)	0.6 (0.0–2.0)		1	2	3
0.9 (0.0–1.6)	0.4 (0.0–0.6)	0.6 (0.0–1.6)		4	2	6
1.0 (0.0–1.8)	0.5 (0.3–0.6)	0.7 (0.0–1.8)		4	1	5

FIG. 3. Normalized *FDXR* gene expression values generated from *in vivo*-irradiated prostate cancer patients are plotted (triangles) left to the *ex vivo in vitro*-generated *FDXR* calibration curve (gray circles) in laboratories 1 (panel A) and 2 (panel B). *FDXR* values from the four prostate cancer patients' pre-exposure samples (white triangles) completely separated from the exposed blood samples (gray triangles) in both laboratories. A 6.9/2.3-fold difference of *in vivo* pre-exposure *FDXR* values relative to the nonirradiated *ex vivo in vitro FDXR* values was applied as a correction factor for the *FDXR* values measured in the exposed prostate cancer patient blood samples and corresponding dose estimates were calculated using the *ex vivo in vitro* calibration curve.

similarly regulated among different individuals compared to, for example, the cell cycle control through a gene such as CDKN1A, which according to our gene expression measurements comprises a higher interindividual variance than *FDXR*.

These features made *FDXR* the most promising candidate for high-throughput biological dosimetry, and even those gene signatures comprising up to 247 genes provided no better dose estimates in our study (Tables 2 and 7). However, it must be noted that the number of samples that could be used for class prediction analysis of microarray features was very low in this study. A low sample-to-feature ratio is an inherent problem for this kind of analysis. In previous studies, gene as well as exon signatures were reported to be very good predictors of radiation dose sensitivity *in vitro* (*6, 9*)[4] as well as *in vivo* (*5*).

In our study we also measured the report time for dose estimates. Again, in agreement with previous work, a period of 7 h was required for dose estimates of 10 blind samples using qRT-PCR (*11*). However, when microarrays were utilized, more than one day was required for the earliest reports of dose estimates due to the 16 h hybridization time inherent to the microarray methodology. Compared to the costs associated with the one-gene qRT-PCR, microarrays are much more expensive and, therefore, may be less applicable for high-throughput dosimetry.

Nevertheless, whole-genome microarray screening remains an important approach for further identifying gene targets/signatures that, to date, remain unidentified. This was also shown in our current study, since all methods proved to be very successful in dose estimates restricted to

TABLE 8
Numbers of Correctly Reported True Negative (TN), True Positive (TP) and Total Measurements to the Three Binary Groupings of Clinical/Diagnostic/Epidemiological Significance for Each Irradiated Sample per Laboratory, Including All Contributions or a Selection of Them

Binary categories of clinical significance	Platform	Measurements			Percentage overall				
		No. of TN	No. of TP	Total	Accuracy	Sensitivity	Specificity	PVP	PVN
Never/ever radiation exposure									
Laboratory 1, all contributions	qRT-PCR	3	23	26	100.0	100.0	100.0	100.0	100.0
Laboratory 2, all contributions	qRT-PCR	3	27	30	100.0	100.0	100.0	100.0	100.0
Laboratory 3, both contributions	Microarray	3	17	20	100.0	100.0	100.0	100.0	100.0
Laboratory 4, above listed 3 contributions	Microarray	3	25	30	93.3	92.6	100.0	100.0	60.0
≤0.2 vs. >0.2 Gy irradiation									
Laboratory 1, all contributions	qRT-PCR	6	20	26	100.0	100.0	100.0	100.0	100.0
Laboratory 2, all contributions	qRT-PCR	6	24	30	100.0	100.0	100.0	100.0	100.0
Laboratory 3, both contributions	Microarray	2	16	20	90.0	100.0	50.0	88.9	100.0
Laboratory 4, above listed 3 contributions	Microarray	6	24	30	100.0	100.0	100.0	100.0	100.0
≤2 vs. >2 Gy irradiation									
Laboratory 1, all contributions	qRT-PCR	13	6	26	73.1	54.5	86.7	75.0	72.2
Laboratory 2, all contributions	qRT-PCR	14	5	30	63.3	33.3	93.3	83.3	58.3
Laboratory 3, both contributions	Microarray	9	6	20	75.0	60.0	90.0	85.7	69.2
Laboratory 4, above listed 3 contributions	Microarray	13	9	30	73.3	60.0	86.7	81.8	68.4

Note. Columns on the right show the agreement in percentage by calculating overall accuracy, sensitivity specificity, PVP and PVN.

TABLE 9
Reported Exposure Status [Unexposed (Unexp) or Exposed (Exp)] as well as Dose Estimates on Four Pre-exposure and Four Exposed Prostate Cancer Patients from Two Laboratories Running qRT-PCR for Each of the Four Prostate Cancer Patients (ID no. 1–4)

Exposure status/true dose for each patient's sample								
Patient ID	1	2	3	4	1	2	3	4
Exposure status	Unexp	Unexp	Unexp	Unexp	Exp	Exp	Exp	Exp
Median radiation dose (Gy)	0	0	0	0	0.01	0.01	0.02	0.01
Mean radiation dose (Gy)	0	0	0	0	0.25	0.32	0.25	0.30

Laboratory/ contribution	Reported exposure/dose estimates (Gy)								Overall			Predictive values	
									Sensitivity (%)	Specificity (%)	agreement (%)	Positive (%)	Negative (%)
Laboratory 1													
FDXR	Unexp	Unexp	Unexp	Unexp	Exp	Exp	Exp	Exp	100.0	100.0	100.0	100.0	100.0
	0.01	0.01	0.01	0.02	0.06	0.07	0.10	0.14					
GADD45	Unexp	Unexp	Exp	Unexp	Exp	Unexp	Exp	Exp	75.0	75.0	75.0	75.0	75.0
	0.00	0.01	0.03	0.02	0.03	0.00	0.03	0.10					
PCNA	Unexp	Unexp	Exp	Exp	Unexp	Unexp	Exp	Exp	50.0	50.0	50.0	50.0	50.0
	0.00	0.01	0.03	0.03	0.01	0.02	0.03	0.20					
Laboratory 2													
FDXR	Unexp	Unexp	Unexp	Unexp	Exp	Exp	Exp	Exp	100.0	100.0	100.0	100.0	100.0
	Unexp	Unexp	Unexp	Unexp	0.08	0.08	0.09	0.08					
PHPT1	Unexp	Unexp	Unexp	Unexp	Exp	Exp	Exp	Exp	100.0	100.0	100.0	100.0	100.0
	0.0	0.0	0.0	0.0	0.0	0.0	0.0	0.04					
DDB2	Unexp	Unexp	Unexp	Unexp	Exp	Exp	Exp	Exp	100.0	100.0	100.0	100.0	100.0
	Unexp	Unexp	Unexp	Unexp	0.0	0.0	0.0	0.0					
CCNG1	Unexp	Unexp	Unexp	Unexp	Exp	Exp	Exp	Exp	100.0	100.0	100.0	100.0	100.0
	0.0	0.0	0.0	0.0	0.0	0.0	0.0	0.0					

Notes. Exposure status and dose estimates are calculated for each laboratory contribution. Measures of sensitivity, specificity, overall agreement, PVP and PVN are calculated based on a 2×2 contingency table depicting the true versus the estimated exposure status.

≤2 Gy, but another analysis algorithm (machine-learning technique) based on the microarray data used in laboratory 4 proved better at predicting doses >2 Gy (Table 7). For this machine-learning technique, we implemented the SMOreg classifier, which implements an SVM for regression and the multilayer perceptron classifier which implements an NN algorithm. To enhance the performance of these learning algorithms we applied two filters: the principal component analysis and correlation-based filters. The correlation-based filter produced a subset of 10 exons related to 5 genes (GADD45A, LRP5, MAMDC4, NDUFAF6, *FDXR*) that were used for the exon-based dose estimates. Using the principal component analysis filter, a subset of 5 genes (*FDXR*, TNFSF8, GADD45A, MDM2, PRKAB1) was identified for the gene-based dose estimates.

From a dosimetric perspective, dose estimates should be as accurate as possible, however, from a clinical perspective, dose ranges are often sufficiently precise for meeting urgent clinical or diagnostic needs. Therefore, to check whether our methodology would be sufficient for triage purposes, we divided blind samples into binary categories. An almost complete separation of unexposed versus exposed samples as well as those exposed to doses ≤0.2 Gy versus higher doses was found (Table 8). This again underscores the high potential of gene expression measurements for dose estimates, especially in the lower dose range, at least for the set of genes utilized in this analysis.

Our *in vivo* approach, using paired blood samples taken before irradiation and 24 h after the first fraction of local radiotherapy to the pelvic region from four prostate cancer patients, confirmed the dose discrimination ability of the gene set already used for the *ex vivo in vitro* part of the study. Again, *FDXR* completely distinguished the pre-exposure samples from the exposed samples, which was probably due to the low interindividual gene expression variance inherent to this gene. These results were found in both qRT-PCR laboratories that contributed to this study. Adjustments for *FDXR* measurements in *in vivo* versus *in vitro* cell culture models differed between both contributing qRT-PCR laboratories, which might be attributable to differences in RNA isolation protocols. The capacity of gene expression measurements to identify exposed individuals in the absence of a pre-exposure control has been previously addressed by others (6), which confirms our findings. Furthermore, exposures resulting in low median/mean equivalent whole-body doses (0.01–0.02/0.25–0.33 Gy) could be discriminated from unexposed samples, which again is a strength of the gene set used.

Finally, we compared *in vivo* with *ex vivo in vitro* gene expression measurements. As could be expected in the absence of cell turnover *in vitro*, gene expression levels were several-fold higher in nonirradiated samples *in vitro* compared to *in vivo* pre-exposure blood samples in the following (shown in parentheses for laboratory 1/laboratory 2): *FDXR* (6.9/2.3-fold), GADD45 (6.8-fold), PCNA (3.0-fold), PHPT1 (1.1-fold), DDB2 (4.1-fold) and CCNG1 (3.6-fold). These ratios

were used as a correction factor for the *in vivo* gene expression measurements in the post-exposure blood samples of prostate cancer patients. The different correction factors observed in both laboratories might reflect methodological discrepancies in the RNA isolation and the qRT-PCR (e.g., normalization). After this adjustment we observed a close agreement of the predicted dose with the individual equivalent whole-body doses estimated based on physical assumptions. However, in general biodosimetry values were higher (Table 9) compared to the median physical dose estimates, an effect which was reproducibly seen in two independent experiments of two different qRT-PCR laboratories. Median values of physical dose reconstructions, as shown in Table 9, appeared more reliable from the physical point of view, but mean values of physical dose reconstruction were about 10 times higher and in better agreement with our biodosimetry data (Table 9). To our knowledge, this is the first time that *in vivo* data were successfully adjusted to *in vitro* measurements, indicating its potential as a strategy to generate dose estimates using *ex vivo in vitro* calibration curves. However, additional studies are needed beyond the four paired blood examinations in this work, to strengthen this finding. Comparisons of *in vivo* with *ex vivo in vitro* gene expression measurements are rare, but similarities in radiation-induced stress-gene expression patterns have been reported (15). To address the differences in, for example, gene copy numbers measured *in vivo* and *in vitro*, we attempted to identify the blood cell counts where the gene expression originated from. However, the small data set presented a challenge to this effort, and therefore, in the absence of these data we assumed that differences in the cell turnover could be best explained by the fold differences observed in our study. Amundson *et al.* used *ex vivo*-irradiated human peripheral blood as a model for *in vivo* irradiation, and reported a signature of 74 genes suitable for dose assessment (0, 0.5, 2, 5 and 8 Gy) at 6–24 h after exposure (6). This classifier predicted certain dose categories in whole-body irradiated patients in the context of another study (16). Using classifiers consisting of several dozens or even hundreds of genes certainly represents another strategy of predicting dose categories and is complementary to the approach shown herein.

Because of the potential challenges involved in comparing gene expression changes after partial *in vivo* exposures with total whole-blood irradiation *in vitro*, for this study we compared an *in vivo* exposure with a well established *in vitro* model. With the introduction of a correction factor both models revealed comparable dose estimates. Assuming that partial-body exposure would change and that the correction factor would also probably change, the *in vitro* model for dose estimates could be still used. That is the potential of our findings, although further studies are needed to support this.

This study has certain strengths and limitations. Considering high-throughput platforms for peripheral blood RNA isolation (e.g., QIAsymphony, Qiagen) combined with 384-well low-density arrays or the 12K open array qRT-PCR platform from Life Technologies about 140 samples could

be processed per day. From a biodosimetry perspective, that represents a new dimension in high sample throughput. Another strength of the gene set examined is the ability to estimate doses ≤2 Gy very accurately. Dose estimates at higher doses become imprecise, which might be avoided using another gene set, as indicated by certain published studies that examined gene signatures *in vivo* (*17*). Blood samples were processed after an incubation period of only 24 h. It is unclear whether the examined genes or another gene set might serve as better candidates for a dose estimate at another point in time after exposure, as some genes are ''early'' radiation-responsive genes and good for early time points while others are ''late'' radiation-responsive genes (*8, 17, 18*). It is unlikely that a single gene might represent a specific response to ionizing radiation and other research is already underway to identify radiation-specific gene signatures that are independent of time after exposure (*9*) and are also not altered by other common factors such as smoking, gender, diseases (sepsis) and chemotherapy (*17, 19*). In addition, dose rate has an effect on gene expression (*20*), and in the event of a nuclear accident most individuals would be nonuniformly exposed to radiation due to partial shielding. However, it has been reported that a partial-body irradiation, even to a single limb, generates a characteristic gene expression signature of radiation injury (*21*). In other words, gene expression can be influenced by many factors and therefore, accurate dose estimations in an actual radiation accident will be complex. Focusing on a gene-to-disease instead of a dose-to-gene association might provide an alternative approach, and in this case, whether the gene(s) became altered due to radiation exposure or other factors would be of less importance. It is important to keep in mind that, initially, predicting health risks based on dose estimates and not on the estimation of the dose itself was the reason for introducing the dose concept.

In summary, fast (7 h for the earliest dose estimates) and precise dose estimates could be performed in particular for doses ≤2 Gy. Moreover, blood samples from prostate cancer patients undergoing radiotherapy could be completely discriminated from pre-exposure blood samples using no calibration curves or any kind of control samples. In addition, dose estimates for these patients based on *in vitro*-generated calibration curves could be successfully performed when the appropriate gene is used and after the *in vivo* gene expression data is adjusted to the artificial *in vitro* situation, characterized by, for example, missing cell turnover. We believe our approach may provide a strategy for estimating doses of *in vivo*-exposed blood samples, by using *ex vivo in vitro*-generated calibration curves.

SUPPLEMENTARY INFORMATION

Table S1. Summary of qRT-PCR data (raw Ct values, transformed Ct values on a linear scale and normalized Ct values) of both qRT-PCR laboratories involved in this exercise.

REFERENCES

1. Chaudhry MA. Biomarkers for human radiation exposure. J Biomed Sci 2008; 15:557–63.
2. IAEA. Cytogenetic analysis for radiation dose assessment: a manual. IAEA Technical Reports Series No. 405. Vienna: International Atomic Energy Agency; 2011. (bit.ly/1JFHWFe)
3. Rothkamm K, Beinke C, Romm H, Badie C, Balagurunathan Y, Barnard S. Comparison of established and emerging biodosimetry assays. Radiat Res 2013; 180:111–19.
4. Amundson SA, Do KT, Shahab S, Bittner M, Meltzer P, Trent J, et al. Identification of potential mRNA biomarkers in peripheral blood lymphocytes for human exposure to ionizing radiation. Radiat Res 2000; 154:342–6.
5. Dressman HK, Muramoto GG, Chao NJ, Meadows S, Marshall D, Ginsburg GS, et al. Gene expression signatures that predict radiation exposure in mice and humans. PLoS Med 2007; 4:e106.
6. Paul S, Amundson SA. Development of gene expression signatures for practical radiation biodosimetry. Int J Radiat Oncol Biol Phys 2008; 71:1236–44.
7. Brengues M, Paap B, Bittner M, Amundson S, Seligmann B, Korn R, et al. Biodosimetry on small blood volume using gene expression assay. Health Phys 2010; 98:179–85.
8. Kabacik S, Mackay A, Tamber N, Manning G, Finnon P, Paillier F, et al. Gene expression following ionising radiation: identification of biomarkers for dose estimation and prediction of individual response. Int J Radiat Biol 2011; 87:115–29.
9. Boldt S, Knops K, Kriehuber R, Wolkenhauer O. A frequency-based gene selection method to identify robust biomarkers for radiation dose prediction. Int J Radiat Biol 2012; 88:267–76.
10. Knops K, Boldt S, Wolkenhauer O, Kriehuber R. Gene expression in low- and high-dose-irradiated human peripheral blood lymphocytes: possible applications for biodosimetry. Radiat Res 2012; 178:304–12.
11. Badie C, Kabacik S, Balagurunathan Y, Bernard N, Brengues M, Faggioni G. Laboratory intercomparison of gene expression assays. Radiat Res 2013; 180:138–48.
12. El-Saghire H, Vandevoorde C, Ost P, Monsieurs P, Michaux A, De Meerleer G, et al. Intensity modulated radiotherapy induces pro-inflammatory and pro-survival responses in prostate cancer patients. Int J Oncol 2014; 44:1073–83.

13. Grace MB, McLeland CB, Blakely WF. Real-time quantitative RT-PCR assay of GADD45 gene expression changes as a biomarker for radiation biodosimetry. Int J Radiat Biol 2002; 78:1011–21.

14. 14. Liu G1, Chen X. The ferredoxin reductase gene is regulated by the p53 family and sensitizes cells to oxidative stress-induced apoptosis. Oncogene 2002; 17:7195–204.

15. Amundson SA, Grace MB, McLeland CB, Epperly MW, Yeager A, Zhan Q, et al. Human in vivo radiation-induced biomarkers: gene expression changes in radiotherapy patients. Cancer Res 2004; 64:6368–71.

16. Paul S, Barker CA, Turner HC, McLane A, Wolden SL, Amundson SA. Prediction of in vivo radiation dose status in radiotherapy patients using ex vivo and in vivo gene expression signatures. Radiat Res 2011; 175:257–65.

17. Meadows SK, Dressman HK, Muramoto GG, Himburg H, Salter A, Wei Z, et al. Gene expression signatures of radiation response are specific, durable and accurate in mice and humans. PLoS One 2008; 3:e1912.

18. Manning G, Kabacik S, Finnon P, Bouffler S, Badie C. High and low dose responses of transcriptional biomarkers in ex vivo x-irradiated human blood. Int J Radiat Biol 2013; 89:512–22.

19. Paul S, Amundson SA. Gene expression signatures of radiation exposure in peripheral white blood cells of smokers and non-smokers. Int J Radiat Biol 2011; 87:791–801.

20. Ghandhi SA, Smilenov LB, Elliston CD, Chowdhury M, Amundson SA. Radiation dose-rate effects on gene expression for human biosimetry. BMC Med Genomics 2015; 8:22.

21. Meadows SK, Dressman HK, Daher P, Himburg H, Russell JL, Doan P, et al. Diagnosis of partial body radiation exposure in mice using peripheral blood gene expression profiles. PLoS One 2010; 5:e11535.